Diabetologia (2013) 56:856–866
DOI 10.1007/s00125-012-2824-6

ARTICLE

Molecular basis for the regulation of islet beta cell mass in mice: the role of E-cadherin

N. Wakae-Takada · S. Xuan · K. Watanabe · P. Meda · R. L. Leibel

Received: 14 August 2012 / Accepted: 13 December 2012 / Published online: 26 January 2013

Abstract
Aims/hypothesis In rodents and humans, the rate of beta cell proliferation declines rapidly after birth; formation of the islets of Langerhans begins perinatally and continues after birth. Here, we tested the hypothesis that increasing levels of E-cadherin during islet formation mediate the decline in beta cell proliferation rate by contributing to a reduction of nuclear β-catenin and D-cyclins.
Methods We examined E-cadherin, nuclear β-catenin, and D-cyclin levels, as well as cell proliferation during in vitro and in vivo formation of islet cell aggregates, using β-TC6 cells and transgenic mice with green fluorescent protein (GFP)-labelled beta cells, respectively. We tested the role of E-cadherin using antisense-mediated reductions of E-cadherin in β-TC6 cells, and mice segregating for a beta cell-specific E-cadherin knockout (*Ecad* [also known as *Cdh1*] βKO).
Results In vitro, pseudo-islets of β-TC6 cells displayed increased E-cadherin but decreased nuclear β-catenin and cyclin D2, and reduced rates of cell proliferation, compared with monolayers. Antisense knockdown of E-cadherin increased cell proliferation and levels of cyclins D1 and D2. After birth, beta cells showed increased levels of E-cadherin, but decreased levels of D-cyclin, whereas islets of *Ecad* βKO mice showed increased levels of D-cyclins and nuclear β-catenin, as well as increased beta cell proliferation. These islets were significantly larger than those of control mice and displayed reduced levels of connexin 36. These changes correlated with reduced insulin response to ambient glucose, both in vitro and in vivo.
Conclusions/interpretation The findings support our hypothesis by indicating an important role of E-cadherin in the control of beta cell mass and function.

Keywords Beta cell signal transduction · Genetics of type 2 diabetes · Islet development

Abbreviations

CDH2	Cadherin 2
CDH5	Cadherin 5, type 2 (vascular endothelium)
ChIP	Chromatin immunoprecipitation
CX36	Connexin 36
E	Embryonic day
Ecad βKO	Beta cell-specific E-cadherin knockout
GFP	Green fluorescent protein
GSIS	Glucose-stimulated insulin secretion
IPGTT	Intraperitoneal glucose tolerance test
PECAM	Platelet/endothelial cell adhesion molecule 1
si	Small interfering
Wnt	Wingless-type MMTV integration site family
WT	Wild-type

Introduction

Relative or absolute deficiency of pancreatic beta cell mass underlies the pathogenesis of type 2 and type 1 diabetes [1].

Electronic supplementary material The online version of this article (doi:10.1007/s00125-012-2824-6) contains peer-reviewed but unedited supplementary material, which is available to authorised users.

N. Wakae-Takada · K. Watanabe · R. L. Leibel
Department of Pediatrics, Columbia University,
New York, NY, USA

N. Wakae-Takada · K. Watanabe · R. L. Leibel (✉)
Naomi Berrie Diabetes Center, Russ Berrie Medical Science Pavilion, 1150 St Nicholas Ave, Suite 620,
New York, NY 10032, USA
e-mail: rl232@columbia.edu

S. Xuan
Department of Genetics and Development, Columbia University,
New York, NY, USA

P. Meda
Department of Cell Physiology and Metabolism,
University of Geneva, Geneva, Switzerland

Among the factors affecting postnatal beta cell mass (i.e. beta cell proliferation, beta cell size, beta cell apoptosis, islet cell transdifferentiation and islet neogenesis) [2], proliferation is considered to be quantitatively the most significant in both humans and mice [3, 4].

In each species, the rate of beta cell proliferation declines after birth [2, 3], reflecting a decrease in the number of cells going through the G1/S transition [5, 6]. Genes that control this transition, such as cyclin D1/D2 and *Cdk4*, influence beta cell proliferation in mouse models [5]. In murine islets, cyclin D2 shows the highest levels compared with other D-cyclins, and plays a primary role in regulating postnatal beta cell mass [7]. From postnatal (P)4 to P10, the percentage of beta cells producing cyclin D2 is reduced threefold, but how and why this decrease occurs is unknown. In mice, formation of the islets of Langerhans begins at embryonic day (E)17.5–E18 [8] and continues after birth until at least P13 [9]. We hypothesised that the cell adhesion molecule, E-cadherin, might be upregulated in response to the cell–cell contacts that beta cells establish during islet formation, contributing to the reduction of cyclin D2, and consequently slowing beta cell replication.

E-cadherin is produced endogenously by beta cells, and mediates most of the Ca^{2+}-dependent cell adhesion between all islet cell types [10]. Overexpression of a dominant-negative form of E-cadherin in beta cells disrupts islet formation at E17.5 [11], and antibodies against E-cadherin prevent pseudo-islet formation in MIN6 cells [12]. E-cadherin has been reported to modify wingless-type MMTV integration site family (Wnt) signalling by tethering β-catenin to the plasma membrane, inhibiting its translocation to the nucleus and thereby decreasing levels of D-cyclin [13].

We also tested the effect of E-cadherin on insulin secretion, as the levels of E-cadherin at the beta cell membrane correlate with insulin secretion [14] by a still-undetermined mechanism that likely involves changes in the gap junction protein connexin 36 (CX36) [15–17].

Here, we report that: (1) the levels of E-cadherin protein increase during pseudo-islet formation in vitro and islet morphogenesis in vivo, in parallel with a decrease in the levels of D-cyclin; (2) loss of E-cadherin production in beta cells, after conditional knockout, is associated with increased beta cell proliferation and beta cell mass; and (3) the increased mass of beta cells resulting from loss of E-cadherin expression is associated with reduced glucose-stimulated insulin release both in vivo and in vitro, consistent with the parallel downregulation of CX36.

Methods

Tissue culture For details of tissue culture, pseudo-islet formation, and transfection for β-TC6 cells, see the electronic supplementary material (ESM) Methods.

Mice The preparation of *Ins2-Gfp* knock-in mice, generated to label beta cells with green fluorescent protein (GFP), is described in the ESM Methods. To generate beta cell-specific E-cadherin knockout mice, *Ins-Cre* mice on a Black Swiss background [18] were crossed with mice with *LoxP* sites flanking exons 6-10 of E-cadherin (B6.129-*Cdh1*^{tm2Kem}/J, *Ecad* [also known as *Cdh1*]$^{fl/fl}$ [19]; Jackson Laboratories, Bar Harbor, ME, USA). See the ESM Methods for further details.

Histology Paraffin sections or cryosections of pancreases were prepared using standard techniques. Histological sections and antibodies used for each histology analysis are described in the ESM Methods.

Western blotting Proteins were extracted using mammalian protein extraction reagents (M-PER) or nuclear and cytoplasmic extraction reagents (NE-PER) (Fisher, Waltham, MA, USA) from whole-cell extracts and purified cytosolic and nuclear fractions, and assayed as described previously [20]. See the ESM Methods for further details.

RNA extraction, cDNA synthesis, quantitative PCR, chromatin immunoprecipitation for β-TC6 cells and isolated islets Total RNA from β-TC6 cells and isolated islets was extracted using the RNeasy kit (Life Technologies, Carlsbad, CA, USA) and cDNA was prepared using SuperScript III (Life Technologies). See the ESM Methods for further details of chromatin immunoprecipitation (ChIP) assay, quantitative PCR and primer sequences.

Cell proliferation assays Cell proliferation was assessed by the following methods: (1) 5-ethylnyl-2′-deoxyuridine (EdU) incorporation, using the Click-iT EdU Flow Cytometry Assay Kit (Life Technologies); (2) fluorescein succinimidyl ester (CFSE; Life Technologies) labelling; (3) BrDU incorporation, quantified using a BrdU ELISA kit (Roche, Indianapolis, IN, USA); and (4) Ki67 immunostaining of primary beta cells. See the ESM Methods for further details.

Cx36 expression and function β-TC6 cells were co-transfected with small interfering (si)RNA against E-cadherin, and with either a green or red fluorescence siGLO Transfection Indicator (Fisher), as described above. After 3 days, cells were either tested by microinjection of ethidium bromide or Lucifer Yellow to assess the functions of CX36 channels, or FACS sorted and then extracted for protein analysis. Detailed methods are provided in the ESM Methods.

Quantification of E-cadherin and cyclin D1/D2 in beta cells from mice of different ages Male mice homozygous for the *Ins2-Gfp* allele were crossed with female C57BL/6J mice. Pancreases of mice at different ages were dissociated into cells

as previously described [21] to quantify E-cadherin and cyclin D1/D2 per beta cell. See the ESM Methods for further details.

Islet isolation and glucose-stimulated insulin secretion Pancreatic perfusion, islet collection, and glucose-stimulated insulin secretion (GSIS) were performed as previously described [20]. Media insulin concentration and the insulin content of the islets were measured using an ultrasensitive mouse insulin ELISA (Mercodia, Uppsala, Sweden). Islet insulin release was expressed in relation to islet insulin content. Islet glucagon concentration was measured using a rat glucagon ELISA (Wako, Richmond, VA, USA).

Islet morphometry Islet morphometric analysis was performed as described by Dokmanovic-Chouinard et al [20]. The insulin-positive area was quantified using ImageProPlus software version 6.3 (Media Cybernetics, Bethesda, MD, USA) and Photoshop CS2 (Adobe, San Jose, CA, USA). Beta cell mass was obtained by multiplying the total pancreas mass (mg) by the mean proportion of insulin-positive area per section and area. The platelet/endothelial cell adhesion molecule 1 (PECAM)- and cadherin 5, type 2 (vascular endothelium) (CDH5 [VE-cadherin])-positive area was expressed as a percentage of total insulin-positive area.

Transmission electron microscopy Batches of 20–30 islets isolated from four control and four beta cell-specific E-cadherin knockout (*Ecad* βKO) mice were processed as described in Stefan et al [22]. Some experiments also investigated control and *Ecad* βKO islets in situ, after similar processing of fragments of intact pancreas (three mice per group). Three to five islets were screened per animal, and about 50 isolated beta cells were screened (three mice per group), under blinded conditions, for potential differences in intercellular junctions between control and *Ecad* βKO mice [23]. Organelles were identified as previously reported [22, 23].

Studies of glucose homeostasis For studies of glucose homeostasis, intraperitoneal glucose tolerance tests (IPGTTs), capillary blood glucose and serum insulin assays, and insulin tolerance tests (ITTs) were performed. See the ESM Methods for further details.

Statistics Student's *t* tests (two-tailed) were performed using Microsoft Excel (Office 2007 and Office 2010). A p value <0.05 was considered significant.

Results

E-cadherin negatively regulates D-cyclin levels and cell proliferation in vitro To assess the effects of aggregation of insulin-producing cells on their proliferation, we generated in vitro islet-like aggregates (pseudo-islets) using SV-40 transformed insulinoma β-TC6 cells. See ESM Results for details. In β-TC6 pseudo-islets, the amount of E-cadherin correlated negatively with the levels of cyclin D2 and cell proliferation rates (ESM Fig. 1a–f). Monolayers of β-TC6 cells treated with an siRNA that reduced *Ecad* mRNA by 90% showed increased cyclin D1 and D2 mRNA and cell proliferation (ESM. Fig. 2a–d). Chromatin immunoprecipitation (ChIP) in cells stably overexpressing E-cadherin showed decreased levels of β-catenin binding to the promoter regions of both cyclin D1 (−50%) and *c-Myc* (also known as *Myc*) (−40%), compared with β-TC6 cells stably transfected with an empty vector (ESM Fig. 2). These observations indicate that the change in beta cell proliferation induced by E-cadherin may be mediated by alterations in the binding of β-catenin to several target genes.

In vivo islet formation is accompanied by increased production of E-cadherin, and decreased production of nuclear β-catenin and cyclin D2 We generated a mouse co-expressing *gfp* and *Ins2* by homologous-recombination-mediated knock-in of the fluorescent protein at the *Ins2* locus (Fig. 1a). The immunoblot of proteins extracted from islets of homozygous and heterozygous *Ins2-Gfp* mice with an anti-GFP antibody showed a 27 kDa band that was not detected in wild-type (WT) control mice (Fig. 1b). Nearly all (96%) of the insulin-positive beta cells of the *Ins2-gfp* homozygous mice showed GFP labelling (Fig. 1c). GFP was not detected in the brain, kidneys or liver (data not shown). At 1.5 months of age, both homozygous and heterozygous *Ins2-gfp* mice had normal glucose tolerance (Fig. 1d).

The levels of E-cadherin per beta cell increased approximately twofold between birth and P22, remaining constant thereafter, while no such change was observed in non-beta pancreatic cells (Fig. 1e). The mRNA levels of cyclins D1/D2 decreased in parallel between P0 and P45 in FACS-sorted beta cells (Fig. 1f). Compared with the levels observed at birth, the levels of cyclin D2 were reduced by 65% and 82% at P22 and P45, respectively. Transcript abundance of cyclin D1 was ten- to 100-fold lower than that of cyclin D2 [7], making it difficult to detect decreases in cyclin D1 levels.

At P1, almost all beta cells in C57BL6/J animals displayed nuclear staining for β-catenin. As the mice aged, the proportion of beta cells with such staining decreased and nuclear β-catenin was not detected in beta cells at P90 (Fig. 1g). These experiments indicate that, during postnatal in vivo islet formation, E-cadherin abundance is negatively correlated with levels of D-cyclins and nuclear β-catenin.

In vivo knockout of E-cadherin does not markedly affect islet structure To examine the effects of E-cadherin on beta

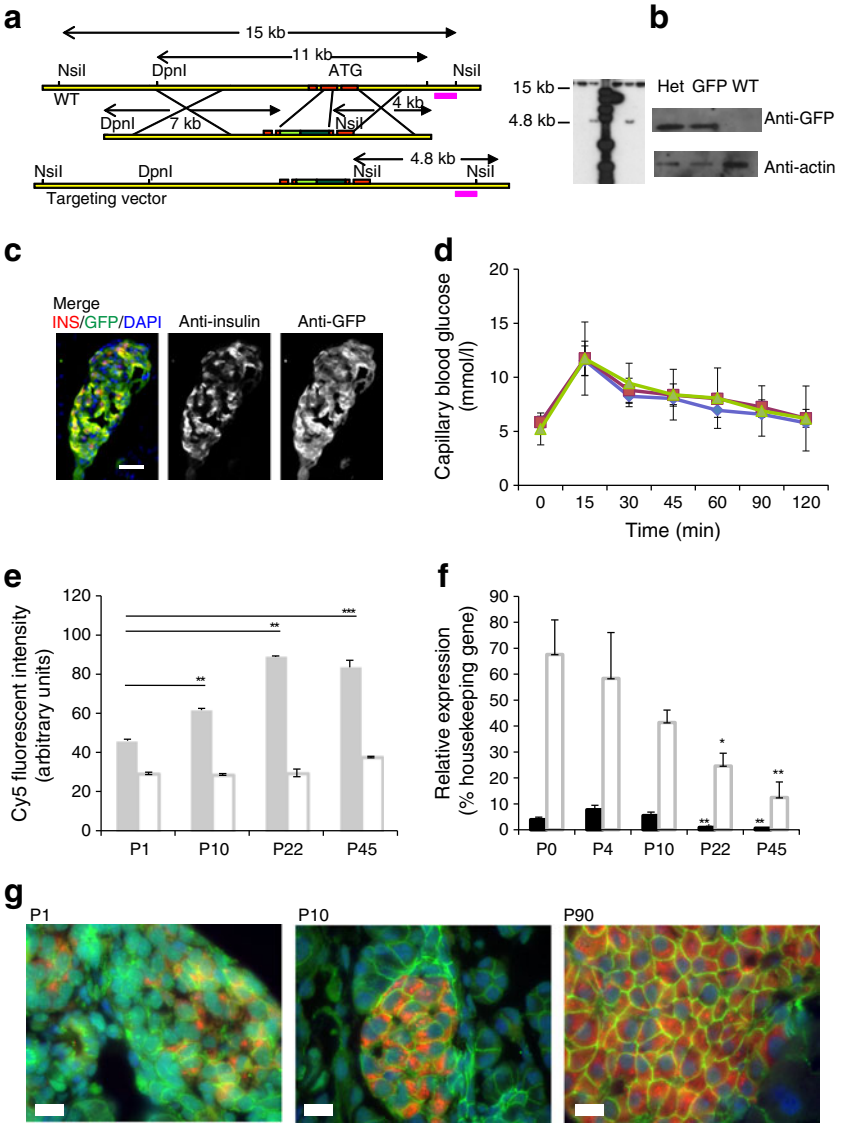

Fig. 1 Construction and analysis of the *Ins2-gfp* knock-in mice. (**a**) Schematic view of the *Ins2-gfp* knock-in construct and Southern blot of embryonic stem cell genomic DNA digested with NsiI, using as probe a 1 kb DNA fragment outside of the 3′ arm of the described construct (pink bars). The probe identifies a 4.8 kb fragment, corresponding to the insert in the correct orientation. Red bar, *Ins2* exon; green bar, GFP-coding region; green bar, kanamycin resistance cassette; ATG, start codon. (**b**) Western blot of total protein extract of isolated islets showing GFP production in the *Ins2-gfp* heterozygous *Ins2-gfp*$^{/+}$ ('Het') and homozygous *Ins2-gfp*/*Ins2-gfp* ('GFP') mouse islets. Actin was used as loading control. (**c**) Fluorescence micrograph of an islet from a 1-month-old *Ins2-gfp* knock-in mouse. Anti-GFP antibody, green; insulin, red; and DAPI, blue. The black and white images of anti-insulin and anti-GFP of the merged images are also shown. Bar, 20 μm. (**d**) IPGTT in 1.5 month-old male mice: WT, green; heterozygous, red curve; and homozygous *Ins2-gfp* mice, blue curve. Data are mean±SEM values of five mice per genotype. (**e**) Levels of E-cadherin from P1 to P22 in GFP-positive beta cells (grey bars) and non-beta endocrine cells (white bars). Data are mean±SEM levels of Cy5 fluorescence per beta cell of five mice per age; $^{**}p<0.01$ and $^{***}p<0.001$ for P1 values vs the other time points. Cy5, cyanin 5. (**f**) Quantitative PCR of mRNA for cyclin D1 (black bars) and D2 (white bars) in postnatal GFP-positive beta cells of heterozygous *Ins2-gfp* mice. Data are mean±SEM values of relative expression for five mice per age; $^{*}p<0.05$ and $^{**}p<0.01$ for samples at P0 vs other time points. (**g**) Representative images of β-catenin (green) staining in islets of 1, 10 and 90-day-old C57BL6/J animals. At all ages: insulin, red; DAPI, blue. Bar, 10 μm. INS, insulin

cell proliferation, we generated mice lacking E-cadherin in beta cells by crossing *Ins-Cre* recombinase mice [18] with *Ecad* $^{fl/fl}$ mice [19]. Immunofluorescence staining of pancreatic sections indicated that E-cadherin was not detectable in beta cells of *Ecad* βKO mice (Fig. 2a). A threefold reduction in E-cadherin protein was consistently observed in the islets of *Ecad* βKO animals (Fig. 2b). Immunohistochemistry indicated that the residual amounts of E-cadherin immunoblotted in the islet extracts (Fig. 2b) could be attributed to modest expression in non-beta cells in which *Ins-Cre* did not excise the targeted region of the E-cadherin gene (Fig. 2a).

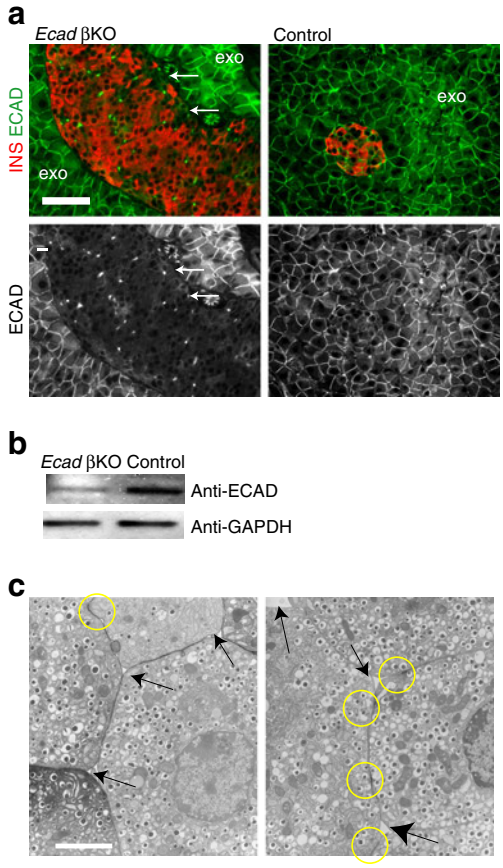

Fig. 2 Histology showing the normal architecture of islets of *Ecad* βKO islets. (**a**) Immunofluorescence staining of 1 month-old pancreas of control *Ins-Cre*:*Ecad*$^{+/+}$ mice (right panels) and *Ecad* βKO mice (left panels). Top panels: E-cadherin, green; insulin, red. Acinar cells are labelled 'exo'. The lower panels are black and white versions of the image. The highly fluorescent green spots dispersed throughout the islet on the top panels are autofluorescent erythrocytes within the islet capillaries. The arrowheads point to non-beta cells immunostained with E-cadherin antibody. Bar, 50 μm in all panels. (**b**) Western blot image of E-cadherin (ECAD) in the islets of *Ecad* βKO mice; 20 μg protein samples were loaded per lane. GAPDH was used as the loading control. (**c**) Electron microscopy of beta cells in islets of *Ecad* βKO (left) and control mice (right). Areas of junctional contacts are circled. The arrowheads point to normal focal regions of enlargement of the intercellular space between beta cells. Bar, 700 nm. ECAD, E-cadherin; INS, insulin

Body weights of *Ins-Cre*:*Ecad*$^{+/+}$ (control) and *Ecad* βKO mice were not significantly different (data not shown). Islets of control and *Ecad* βKO mice did not differ in such ultrastructural features of beta cells as closely apposed plasma membranes (Fig. 2c), the mRNA and protein of beta cell maturation markers (data not shown), and the mRNA of 18 other cadherin species (data not shown). There was no visible change in either the configuration or number of alpha cells (ESM Fig. 3), nor was there a change in islet glucagon content ([mean±SEM]: 1 month-old *Ecad* βKO mice 0.56±383 nmol/μg of DNA; control: 0.54±0.06 nmol/μg; n=4 for each genotype), or mRNA of glucagon in islets (data not shown). However, *Cdh2* and *Cdh5* mRNA increased by nine- and fourfold, respectively, in the islets of *Ecad* βKO animals (Fig. 3a). Immunofluorescence revealed cadherin 2 (CDH2 [N-cadherin]) in the beta cells of *Ecad* βKO mice (Fig. 3b), whereas CDH5 was detected in the islet blood vessels of both *Ecad* βKO and control mice (Fig. 3c). CDH2 abundance was approximately threefold higher (3.0 ±0.50, n=3) in islets of 1 month-old *Ecad* βKO animals than in islets of age-matched controls (Fig. 3d). Consistent with the increased mRNA expression of *Cdh5* in 1 month-old *Ecad* βKO animals, the area immunostained with CDH5 antibody was twofold larger in 1 month-old *Ecad* βKO

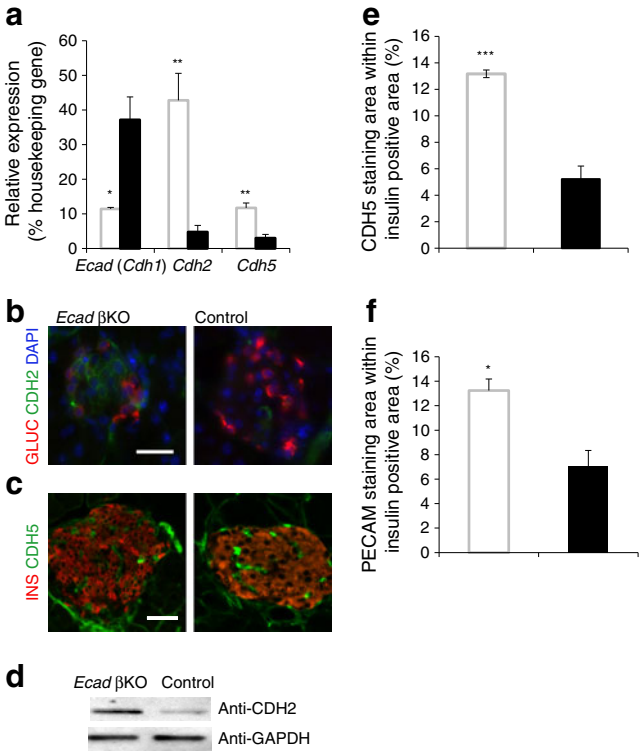

Fig. 3 Loss of E-cadherin is associated with increased expression of other cadherins in islets of 1 month-old *Ecad* βKO mice. (**a**) Quantitative PCR of *Ecad*, *Cdh2* mRNA and *Cdh5* mRNA in islets of 1 month-old *Ecad* βKO (white bars, n=4) and control (black bars, n=4). Data are presented as mean±SEM mRNA expression relative to that of 36B4; $^{*}p<0.05$ and $^{**}p<0.01$ for *Ecad* βKO vs control. (**b**) Confocal micrographs of islets from 1-month-old *Ecad* βKO (left) and control (*Ins-Cre*:*Ecad*$^{+/+}$) mice (right) stained for: CDH2, green; glucagon, red; and DAPI, blue. Bar, 20 μm. (**c**) Immunostaining of CDH5 (green) in control (*Ins-Cre*:*Ecad*$^{+/+}$) (right) or *Ecad* βKO islets (left). Insulin, red. Bar, 50 μm. (**d**) Western blot image of CDH2 (N-cadherin) in the islets of *Ecad* βKO mice and control; 20 μg protein samples were loaded per lane. GAPDH was used as the loading control. (**e**) The area positively stained with CDH5, expressed as the percentage of insulin-positive area, in 1-month-old *Ecad* βKO mice (white bar, n=4) and controls (black bar, n=4). Data are presented as mean±SEM; $^{***}p<0.001$. (**f**) The area positively stained with PECAM, expressed as percentage of insulin-positive area, in 1-month-old *Ecad* βKO mice (white bar, n=4) and controls (black bar, n=4). Data are presented as mean±SEM; $^{*}p<0.05$

animals than in control animals (Fig. 3e). Blood vessel density measured by percentage of area immunostained for PECAM within the insulin-positive area was increased approximately twofold in 1 month-old *Ecad* βKO animals (Fig. 3f), suggesting that the increased level of CDH5 can be accounted for by increased blood vessel density. These observations indicate that in vivo knockout of E-cadherin in beta cells did not markedly alter the organisation of beta cells within the islets, possibly because of compensatory changes in other cadherins.

In vivo knockout of E-cadherin increases beta cell proliferation Immunoblots of islet proteins indicated that cytoplasmic β-catenin was detectable only in *Ecad* βKO islets, and that when these animals were 1 month of age, nuclear β-catenin was increased approximately ninefold (9.3±1.0, n=3) over control levels (Fig. 4a). In islets of 1 month-old *Ecad* βKO mice, cyclin D1 and cyclin D2 mRNA increased (p<0.05) four- and threefold, respectively, vs controls (Fig. 4b). Cyclin D2 protein also increased in the islets of 1 month-old *Ecad* βKO mice (Fig. 4c). These results indicate that the increased beta cell proliferation in *Ecad* βKO animals was associated with increased levels of β-catenin and cyclins D1 and D2.

To estimate the proportions of dividing beta cells, the number of Ki67-positive cells was related to the total number of insulin-positive beta cells [20]. *Ecad* βKO mice showed higher rates of beta cell proliferation vs age-matched control animals. The percentages of Ki67-positive beta cells were 1.5-fold (p=0.05) and twofold (p<0.01) higher in 7 day- and 1 month-old animals, respectively (Fig. 4d). This difference did not reach statistical significance in 3 month-old animals (Fig. 4d) that showed an increase in beta cell mass (Fig. 4e).

E-cadherin knockout decreases glucose tolerance and GSIS Although 1 month-old *Ecad* βKO and control animals have similar glucose tolerance (Fig. 5a), 3 to 4 month-old

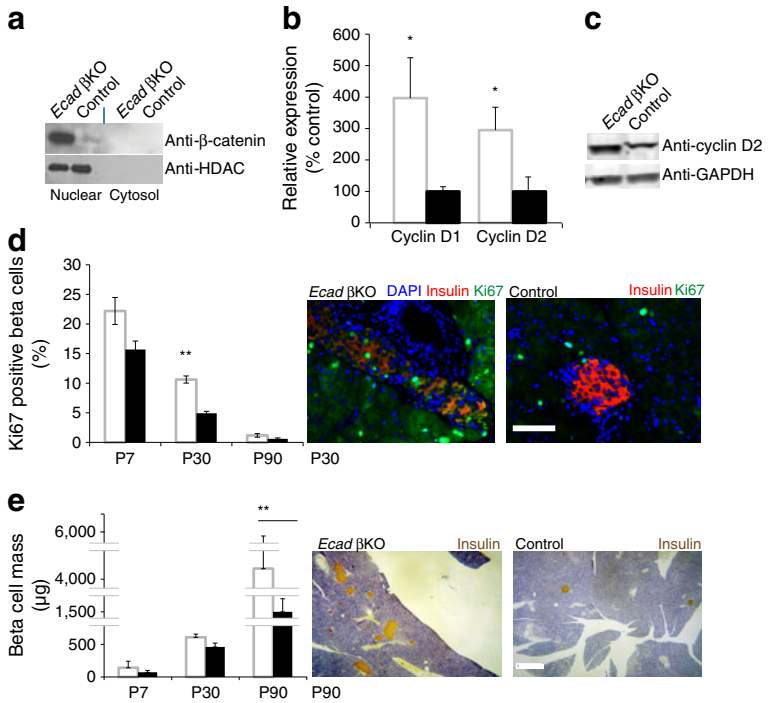

Fig. 4 One-month-old *Ecad* βKO mice showing increased nuclear β-catenin protein, cyclin D1/D2 mRNA expression and beta cell proliferation. (**a**) Western blot image of nuclear and cytosolic proteins from islets of 1-month-old *Ecad* βKO and control (*Ins-Cre*:*Ecad*$^{+/+}$) mice for β-catenin and histone deacetylase (HDAC). Islets from four animals were pooled per genotype, and 20 μg protein samples loaded per lane. (**b**) Quantitative PCR of cyclin D1/ D2 transcripts in islets of 1-month-old *Ecad* βKO mice (white bars, n=6) and in islets of age-matched controls (*Ins-Cre*:*Ecad*$^{+/+}$, black bar, n=5). Data are mean±SEM, normalised to those of the ribosomal housekeeping gene, *36b4*, and shown as percentage of control value (set to 100). $^{*}p$< 0.05: *Ecad* βKO vs controls. (**c**) Western blot image for cyclin D2 in islets of 1 month-old *Ecad* βKO mice and age-matched controls (*Ins-Cre*:*Ecad*$^{+/+}$). (**d**) The proportion of Ki67-positive beta cells in control (*Ins-Cre*:*Ecad*$^{+/+}$, black bars, n=4) and *Ecad* βKO mice (white bars, n=4). Data are mean±SEM; $^{**}p$<0.01 for *Ecad* βKO vs control at P30; p=0.05 and 0.08 for *Ecad* βKO vs control at P7 and P90, respectively. The micrographs panels compare the immunofluorescence staining for Ki67 (green) in the insulin (red)-containing islet cells of *Ecad* βKO (left) and control mice (right). DAPI, blue. Bar, 50 μm. (**e**) The beta cell mass of both control (*Ins-Cre*:*Ecad*$^{+/+}$, black bars) and *Ecad* βKO mice (white bars) at different ages (P7, P30, P90). Values are mean±SEM of beta cell mass; $^{**}p$<0.01 *Ecad* βKO vs controls. The micrographs panels compare the immunostaining for insulin (brown DAB staining) of *Ecad* βKO (left) and control mice (right). Five sections spanning the entire pancreas were analysed in four to five mice per genotype and age. Bar, 100 μm

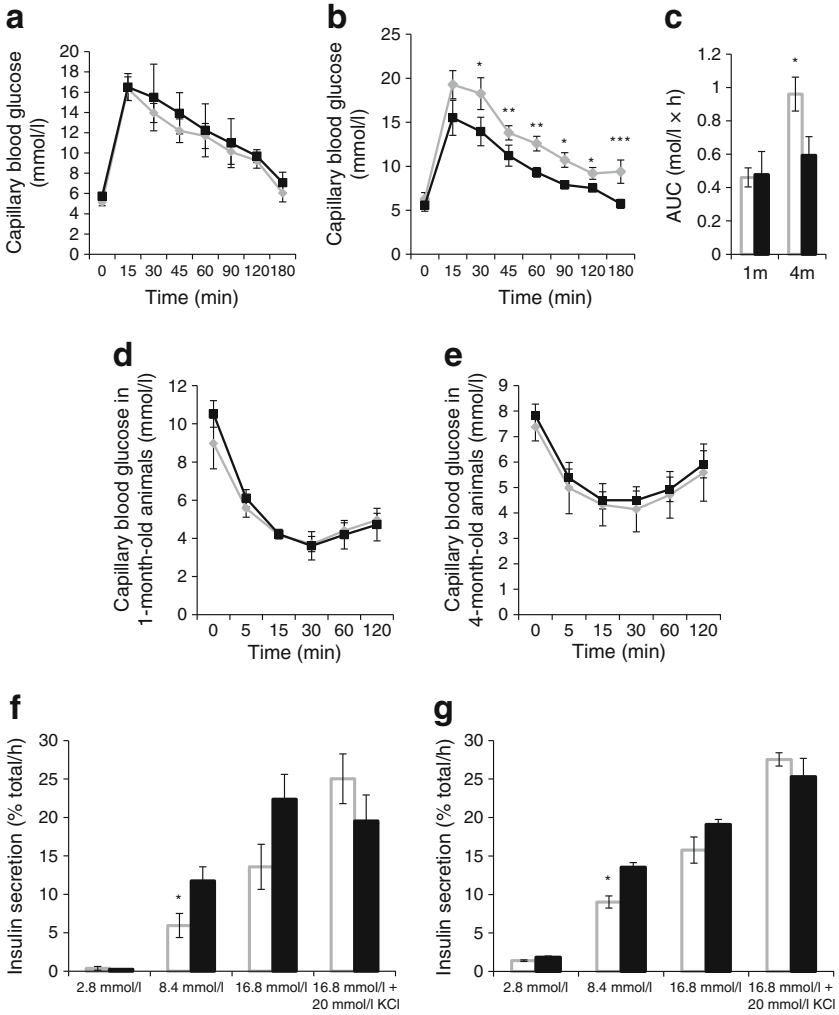

Fig. 5 Adult *Ecad* βKO mice feature glucose intolerance caused by reduced insulin secretion, in the absence of differences in systemic insulin sensitivity. (**a**,**b**) IPGTT in (**a**) 1, and (**b**) 4 month-old *Ins-Cre*:*Ecad*$^{+/+}$ (black line) and *Ecad* βKO animals (grey line) fasted for 18 h. Capillary blood glucose concentrations are presented as mean±SEM for seven to ten mice per genotype and age; $^{*}p<0.05$, $^{**}p<0.01$ and $^{***}p<0.001$. (**c**) Area under the curve analysis for *Ecad* βKO animals (white bars) and control *Ins-Cre*:*Ecad*$^{+/+}$ animals (black bars) at 1 and 4 months of age from the experiments shown in Fig. 5a,b. Data are presented as mean±SEM for seven to ten mice per genotype and age; $^{*}p<0.05$. (**d**,**e**) Capillary blood glucose after i.p. injection of insulin. *Ecad* βKO (grey line) and control mice (*Ins-Cre*:*Ecad*$^{+/+}$, black line) at 1 month (**d**) and 4 months of age (**e**). Capillary blood glucose concentrations are presented as mean±SEM for six to seven mice per genotype and age. (**f**,**g**) GSIS and KCl-stimulated insulin secretion from islets isolated from (**f**) 1, and (**g**) 4 month-old control (*Ins-Cre*:*Ecad*$^{+/+}$, black bars) and *Ecad* βKO animals (white bars). Data are presented as mean±SEM % insulin release normalised by total insulin contents; $^{*}p<0.05$

Ecad βKO mice showed reduced glucose tolerance (Fig. 5b), despite a 2.5-fold increase in beta cell mass and normal levels of several beta cell markers (Fig. 4e and data not shown). Area under the curve analysis confirmed the decreased glucose tolerance in 3 to 4 month-old *Ecad* βKO mice compared with control (Fig. 5c). No differences in insulin sensitivity (by insulin tolerance testing) and fasting insulin levels were apparent in either 1 or 4 month-old animals (Fig. 5d, e and ESM Fig. 4a). In mice at 1 month of age, the serum insulin concentrations after intraperitoneal glucose administration were not different between *Ecad* βKO and control animals (ESM Fig. 4b, c). However, 4 month-old animals displayed lower serum insulin concentrations at time point 15 min of the IPGTT (ESM Fig. 4d, e). Islets isolated from 1- and 4-month-old *Ecad* βKO mice secreted 40% and 50% less insulin, respectively, ($p<0.05$) in response to 8.4 mmol/l glucose (Fig. 5f, g). No difference was observed in the responses of these islets to 2.8 mmol/l glucose, 16.8 mmol/l glucose or 16.8 mmol/l glucose plus 20 mmol/l KCl (Fig. 5f, g). Under all of these conditions, islets of *Ins-Cre* mice displayed insulin secretion rates comparable with those of C57BL6/J controls (ESM Fig. 5). The insulin content of islets from *Ecad* βKO mice (1.7±0.3 μg/g DNA) was not different from that of controls (2.0±0.2 μg/g DNA).

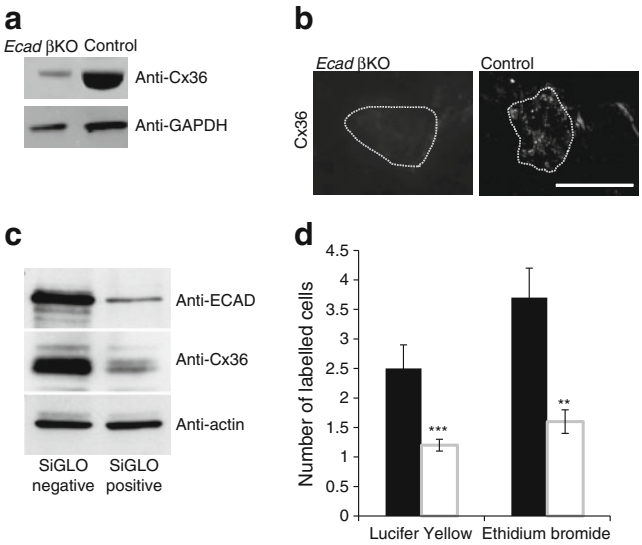

Fig. 6 The expression and function of CX36 is decreased after loss of beta cell E-cadherin both in vivo and in vitro. (**a**) Western blot image for CX36 in 1 month-old *Ecad* βKO islets; 20 μg whole-cell protein extracts were loaded. GADPH was used as the loading control. (**b**) Immunofluorescence staining of frozen sections of pancreas for CX36 within an islet (bounded area) of a control (*Ins-Cre*:*Ecad*$^{+/+}$). Bar, 100 μm. (**c**) Western blot image for CX36 in β-TC6 exposed to siRNA against E-cadherin (siGLO positive) and companion non-transfected β-TC6 (siGLO negative); 10 μg protein/lane. See Methods for further details. Actin was used as the loading control. (**d**) The gap junctional coupling of β-TC6 cells exposed to siRNA against E-cadherin (siGLO positive, white bars, n=14) and companion non-transfected β-TC6 (siGLO negative, black bars, n=10) measured by number of cells labelled by the microinjected tracer. Data are presented as mean± SEM; $^{***}p<0.001$ vs Lucifer Yellow control value; $^{**}p<0.01$ vs ethidium bromide control value

Response to ambient glucose is partly dependent on beta cell to beta cell communication mediated by gap junctions [24, 25]. In islets of *Ecad* βKO mice, there was an approximately 2.5-fold (2.4±0.4, n=2) reduction in levels of CX36 protein (Fig. 6a, b), a critical functional component of beta cell gap junctions [26, 27]. Three days after transfection of β-TC6 cells with an siRNA against E-cadherin, these cells, with an approximate fivefold reduction in E-cadherin levels (5.0±0.22, n=2), also showed an approximate fivefold reduction (4.7±0.2, n=2) in abundance of CX36 protein (Fig. 6c). Microinjection of two gap junction tracers, Lucifer Yellow and ethidium bromide [28], further revealed that the transfected cells containing reduced levels of E-cadherin were also significantly less coupled than cells that escaped transfection (Fig. 6d, Table 1).

Discussion

In mice and humans, beta cell proliferation rates decline postnatally and, at least in mice, this change is associated with a decline in the levels of cyclin D2 [29]. However, the mechanisms that trigger these changes are still a matter of debate. The aggregation of endocrine cells in the proto-islet begins around E17.5, and islet formation continues in the neonatal period [9, 11]. Because of the highly ordered structure of the islets, the well-documented dependence of coordinated endocrine function on both paracrine and contact-dependent communication of the endocrine cells [25, 30, 31], and the role of E-cadherin in mediating relevant aspects of cellular architecture [10, 11], we examined the role of this cell adhesion molecule in the in vivo development and function of beta cells, with particular regard to their insulin secretion and rates of proliferation.

We have found that the production of E-cadherin in beta cells increases both in vivo and in vitro with the formation of islet structures, and is accompanied by decreased levels of D-cyclin, and decreased beta cell proliferation. Our analyses of mice with a null beta cell E-cadherin allele (*Ecad* βKO), as well as of insulin-producing cells with reduced E-cadherin abundance through exposure to a specific siRNA, indicate that E-cadherin negatively regulates beta cell proliferation by reducing the levels of β-catenin in the nucleus, resulting in decreased D-cyclin levels. This inference is consistent with a scenario in which increased levels of E-cadherin, as a result of establishment of cell contacts during islet formation, contributes to the postnatal reduction in beta cell proliferation.

Despite the loss of E-cadherin, beta cells retain apparently normal physical contacts with nearby cells within the islets of *Ecad* βKO mice. Whereas disruption of beta cell apposition has been reported to result from overexpression of a dominant-negative isoform of E-cadherin [11], after incubation of islets with antibodies to E-cadherin [32], or after knockdown of E-cadherin in MIN6 cells [33], others have found that beta cells could still adhere in clusters after reduction of E-cadherin by siRNA or short hairpin (sh)RNA [15, 16]. Presumably, these differences can be accounted for by differences in the residual levels of other cell adhesion molecules, the extent to which the level of E-cadherin is reduced [16], and by compensatory changes in the many proteins that participate in beta to beta cell contacts and adherence. Our data show that these proteins may include CDH2, a molecule that facilitates cell–cell adhesion [34], and CDH5, a class II cadherin that does not heterodimerise with type 1 cadherins such as CDH2. The changes in CDH2 were not observed in β-TC6 cells in which *Ecad* was reduced by siRNA, suggesting that these responses are highly dependent on the context of individual cell types. The increased CDH5 abundance in endothelial cells was associated with an increase in the density of the islet vessels and could conceivably contribute to the sustaining of normal architecture in *Ecad* βKO islets. The reasons for the increase in blood vessel density remain to be determined. In another system, the decrease in islet vascularisation observed as a result of reduced expression of *Sorcs* (also

Table 1 Tracer microinjection indicates reduced intercellular coupling of β-TC6 cells when E-cadherin expression is suppressed

β-TC6 type	Coupling incidence (% injections)[a]		Coupling index[b]		
	Lucifer Yellow	Ethidium bromide	Lucifer Yellow	Ethidium bromide	Total[c] (10^3)
siGLO-positive, si*Ecad* transfected	22	50	26	80	2
siGLO-negative control	70	77	175	285	50

β-TC6 cells were exposed to an siRNA against E-cadherin and to the siGLO fluorescent transfection indicator. After 3 days, successfully transfected cells (siGLO positive) were separated by FACS from companion non-transfected cells (siGLO negative), and analysed for beta cell coupling as described in the Methods; 10–14 microinjections were performed per group

Data are mean±SE

[a] Per cent of injections showing coupling

[b] Mean coupling extent×coupling incidence

[c] Coupling index for Lucifer Yellow×coupling index for ethidium bromide

known as *Sorcs1*) was indeed accompanied by disruption of normal islet architecture [35].

The apparently structurally normal islets of *Ecad* βKO mice contained a larger mass of beta cells than did the islets of control mice. This change was associated with an increase in the proliferation of primary beta cells, consistent with the increased rate of replication observed in β-TC6 cells after reduction of E-cadherin expression by siRNA. In rodents, most new islets form [9, 11] and increase in size [3] during the early postnatal period (P0–P22), during which time the levels of beta cell E-cadherin protein also increase as a result of the establishment of increasing numbers of cell-to-cell contacts within the forming islets [36]. During this period the rate of beta cell proliferation also decelerates [5, 6, 29]. We found that the levels of cyclins D1/D2 in beta cells also decreased from P0 to P22, as did the proportion of nuclear to cytoplasmic β-catenin.

The central question is whether these in vitro and in vivo changes in E-cadherin, β-catenin and cyclins D1/D2 are mechanistically related to the observed developmental changes in beta cell replication rates and function. The data are consistent with a scenario analogous to that of the canonical Wnt pathway [13], in which increased expression of E-cadherin decreases nuclear levels of β-catenin, resulting in downregulation of the key cell proliferation genes, including cyclins D1/D2. These changes would be anticipated to reduce beta cell proliferation, and this prediction was fulfilled by our experiments. Thus, reduced E-cadherin expression, as a result of exposure to specific siRNAs, was associated with increased proliferation of β-TC6 cells. Conversely, increased E-cadherin abundance in β-TC6 pseudo-islets was associated with reduced cyclin D2 levels and a reduced proportion of cells featuring detectable nuclear β-catenin. The latter observation was also made in primary beta cells during the formation of islets between P0 and P90. ChIP assays further showed that increased E-cadherin levels resulted in decreased binding of β-catenin to promoters of known Wnt targets, including cyclin D1 and *c-Myc*.

Our data extend those of previous studies in which conditional pancreas-specific disruption of β-catenin resulted in decreased numbers of beta cells and total islet area at birth [37], whereas levels of a constitutively activated β-catenin in beta cells increased nuclear levels of β-catenin, resulting in increased cyclin D2 levels and beta cell proliferation [38]. However, other studies testing the down- or upregulation of β-catenin expression have suggested that, under some circumstances, this protein may be dispensable for endocrine cell differentiation, proliferation and function [39]. Presumably, differences in the timing and efficiency of the Cre recombinase-dependent activation of the different promoters (pancreatic and duodenal homeobox 1 [PDX1], regulation of phenobarbital-inducible P450 [RIP]), which were used in these studies, account for these somewhat different observations.

It is equally possible that E-cadherin regulates beta cell proliferation by a variety of pathways, only some of which may be independent of β-catenin. We have observed, for example, that increased production of E-cadherin in pseudo-islets is associated with decreased expression of *Ezh2* (data not shown), which encodes a transcription factor involved in the platelet-derived growth factor (PDGF) pathway that enhances beta cell proliferation [40]. Whatever the mechanism(s), it is relevant that the increased beta cell proliferation and mass that we observed in *Ecad* βKO mice was not induced by increased insulin resistance, given that the sensitivity of these animals to an acute insulin challenge was unaffected throughout their postnatal life.

Despite the increased beta cell mass in the islets of *Ecad* βKO mice, these animals were modestly glucose intolerant, as a result of reduced glucose-stimulated release of insulin by their islets. The mechanism of this unexpected functional defect remains to be determined. A discrepancy in insulin responses in 1 month-old *Ecad* βKO animals existed:

normal in vivo and reduced in vitro. These results could reflect an experimental artefact and/or physiologically relevant compensations provided by the in vivo environment. One possible explanation for the discrepancy in insulin secretion in vitro vs in vivo could be that the increased number of blood vessels in vivo facilitated in vivo insulin secretion, compensating for a reduction in insulin secretion per beta cell (reviewed in Eberhard et al [41]).

Our experiments show that the in vivo loss of *Ecad* was associated with a marked decrease in the CX36 protein, consistent with previous data obtained in an insulin-producing cell line [15]. Given that our in vitro experiments further document that such a loss significantly reduced the functional coupling of β-TC6 cells, and that *Cx36* (also known as *Gjd2*) coupling is implicated in the control of GSIS [17, 24, 26, 42], it is plausible that the secretory defects of *Ecad* βKO mice are at least partly dependent on loss of CX36 coupling. In addition, CX36 is required for the effects of the Eph-ephrin pathway on insulin secretion [43]. Therefore, the decrease in insulin secretion in 1 and 4 month-old *Ecad* βKO animals could also be accounted for, in part, by the reduction in the stimulatory activity of Eph-ephrin pathway resulting from the reduced CX36 abundance as a consequence of loss of E-cadherin. Furthermore, the age-dependent phenotype of glucose intolerance observed in 4 month-old *Ecad* βKO animals could also be explained by the decreased stimulatory effect of Eph signalling on GSIS caused by ageing in addition to the increased metabolic 'pressure' on beta cells caused by increased body mass. Increased penetrance of knockout phenotypes with age is commonly observed [43]. At any rate, the observation that the glucose intolerance and loss of glucose-sensitive insulin release became apparent only in adult mice suggests that the relevant mechanism becomes a limiting factor as metabolic demand increases.

In summary, these studies provide evidence that E-cadherin plays a significant physiological role in the postnatal control of beta cell proliferation and function. As E-cadherin is also found in human beta cells [44], it is possible, if not likely, that the cell adhesion molecule also plays a similar role in human beta cells, thereby affecting susceptibility to diabetes. *CDH1*, which encodes human E-cadherin, is located at Chr. 16q22.1, a locus that has been implicated in susceptibility to type 1 diabetes [45].

Acknowledgements The authors thank: D. Accili (Department of Medicine, Columbia University, New York, NY, USA) and L. Sussel (Department of Genetics and Development, Columbia University, New York, NY, USA) for helpful advice throughout this project; A. Efstratiadis (Department of Genetics and Development, Columbia University, New York, NY, USA, currently at the Biomedical Research Foundation, Athens, Greece) for providing the *Ins2-Gfp* mice; D. Caille-Rigo (Department of Cell Physiology and Metabolism, University of Geneva, Geneva, Switzerland); S. G. Fischer for assistance in formatting figures and text; and R. Rausch (Department of Pediatrics, Columbia University, New York, NY, USA) for excellent technical assistance.

Funding This work was supported by NIH DK66518, 5P30DK63608, the Helmsley Trust and the Russell Berrie Foundation Program in Cellular Therapies of Diabetes. PM is supported by grants from the Swiss National Science Foundation (310000-109402, CR32I3_129987, IZ73Z0_127935), the Juvenile Diabetes Research Foundation (40-2011-11), and the European Union (BETAIMAGE 222980; IMIDIA, C2008-T7, BETATRAIN, 289932).

Duality of interest The authors declare that there is no duality of interest associated with this manuscript.

Contribution statement All the authors have: (1) substantially contributed to the conception, design, acquisition of data, and analysis of data; (2) contributed to drafting the manuscript or revising it critically; and (3) approved the final version of the manuscript.

References

1. Butler AE, Janson J, Bonner-Weir S, Ritzel R, Rizza RA, Butler PC (2003) Beta-cell deficit and increased beta-cell apoptosis in humans with type 2 diabetes. Diabetes 52:102–110
2. Rhodes CJ (2005) Type 2 diabetes—a matter of beta-cell life and death? Science 307:380–384
3. Meier JJ, Butler AE, Saisho Y et al (2008) Beta-cell replication is the primary mechanism subserving the postnatal expansion of beta-cell mass in humans. Diabetes 57:1584–1594
4. Dor Y, Brown J, Martinez OI, Melton DA (2004) Adult pancreatic beta-cells are formed by self-duplication rather than stem-cell differentiation. Nature 429:41–46
5. Ackermann AM, Gannon M (2007) Molecular regulation of pancreatic beta-cell mass development, maintenance, and expansion. J Mol Endocrinol 38:193–206
6. Kauri LM, Wang GS, Patrick C, Bareggi M, Hill DJ, Scott FW (2007) Increased islet neogenesis without increased islet mass precedes autoimmune attack in diabetes-prone rats. Lab Invest 87:1240–1251
7. Kushner JA, Ciemerych MA, Sicinska E et al (2005) Cyclins D2 and D1 are essential for postnatal pancreatic beta-cell growth. Mol Cell Biol 25:3752–3762
8. Murtaugh LC (2007) Pancreas and beta-cell development: from the actual to the possible. Development 134:427–438
9. Scaglia L, Cahill CJ, Finegood DT, Bonner-Weir S (1997) Apoptosis participates in the remodeling of the endocrine pancreas in the neonatal rat. Endocrinology 138:1736–1741
10. Rouiller DG, Cirulli V, Halban PA (1991) Uvomorulin mediates calcium-dependent aggregation of islet cells, whereas calcium-independent cell adhesion molecules distinguish between islet cell types. Dev Biol 148:233–242
11. Dahl U, Sjodin A, Semb H (1996) Cadherins regulate aggregation of pancreatic beta-cells in vivo. Development (Cambridge, England) 122:2895–2902
12. Hauge-Evans AC, Squires PE, Persaud SJ, Jones PM (1999) Pancreatic beta-cell-to-beta-cell interactions are required for integrated responses to nutrient stimuli: enhanced Ca2+ and insulin secretory responses of MIN6 pseudoislets. Diabetes 48:1402–1408
13. Nelson WJ, Nusse R (2004) Convergence of Wnt, beta-catenin, and cadherin pathways. Science 303:1483–1487

14. Bosco D, Rouiller DG, Halban PA (2007) Differential expression of E-cadherin at the surface of rat beta-cells as a marker of functional heterogeneity. J Endocrinol 194:21–29
15. Calabrese A, Caton D, Meda P (2004) Differentiating the effects of Cx36 and E-cadherin for proper insulin secretion of MIN6 cells. Exp Cell Res 294:379–391
16. Jaques F, Jousset H, Tomas A et al (2008) Dual effect of cell-cell contact disruption on cytosolic calcium and insulin secretion. Endocrinology 149:2494–2505
17. Meda P (2012) The in vivo beta-to-beta-cell chat room: connexin connections matter. Diabetes 61:1656–1658
18. Herrera PL (2000) Adult insulin- and glucagon-producing cells differentiate from two independent cell lineages. Development 127:2317–2322
19. Boussadia O, Kutsch S, Hierholzer A, Delmas V, Kemler R (2002) E-cadherin is a survival factor for the lactating mouse mammary gland. Mech Dev 115:53–62
20. Dokmanovic-Chouinard M, Chung WK, Chevre JC et al (2008) Positional cloning of "Lisch-Like", a candidate modifier of susceptibility to type 2 diabetes in mice. PLoS Genet 4:e1000137
21. White P, May CL, Lamounier RN, Brestelli JE, Kaestner KH (2008) Defining pancreatic endocrine precursors and their descendants. Diabetes 57:654–668
22. Stefan Y, Meda P, Neufeld M, Orci L (1987) Stimulation of insulin secretion reveals heterogeneity of pancreatic B cells in vivo. J Clin Investig 80:175–183
23. Sumara G, Formentini I, Collins S et al (2009) Regulation of PKD by the MAPK p38delta in insulin secretion and glucose homeostasis. Cell 136:235–248
24. Bosco D, Haefliger JA, Meda P (2011) Connexins: key mediators of endocrine function. Physiol Rev 91:1393–1445
25. Meda P (1996) The role of gap junction membrane channels in secretion and hormonal action. J Bioenerg Biomembr 28:369–377
26. Ravier MA, Guldenagel M, Charollais A et al (2005) Loss of connexin36 channels alters beta-cell coupling, islet synchronization of glucose-induced Ca2+ and insulin oscillations, and basal insulin release. Diabetes 54:1798–1807
27. Theis M, Mas C, Doring B et al (2004) Replacement by a lacZ reporter gene assigns mouse connexin36, 45 and 43 to distinct cell types in pancreatic islets. Exp Cell Res 294:18–29
28. Charpantier E, Cancela J, Meda P (2007) Beta cells preferentially exchange cationic molecules via connexin 36 gap junction channels. Diabetologia 50:2332–2341
29. Georgia S, Bhushan A (2004) Beta cell replication is the primary mechanism for maintaining postnatal beta cell mass. J Clin Invest 114:963–968
30. Gromada J, Franklin I, Wollheim CB (2007) Alpha-cells of the endocrine pancreas: 35 years of research but the enigma remains. Endocr Rev 28:84–116
31. Luther MJ, Davies E, Muller D et al (2005) Cell-to-cell contact influences proliferative marker expression and apoptosis in MIN6 cells grown in islet-like structures. Am J Physiol Endocrinol Metab 288:E502–509
32. Yamagata K, Nammo T, Moriwaki M et al (2002) Overexpression of dominant-negative mutant hepatocyte nuclear fctor-1 alpha in pancreatic beta-cells causes abnormal islet architecture with decreased expression of E-cadherin, reduced beta-cell proliferation, and diabetes. Diabetes 51:114–123
33. Carvell MJ, Marsh PJ, Persaud SJ, Jones PM (2007) E-cadherin interactions regulate beta-cell proliferation in islet-like structures. Cell Physiol Biochem 20:617–626
34. Matsunaga M, Hatta K, Takeichi M (1988) Role of N-cadherin cell adhesion molecules in the histogenesis of neural retina. Neuron 1:289–295
35. Clee SM, Yandell BS, Schueler KM et al (2006) Positional cloning of Sorcs1, a type 2 diabetes quantitative trait locus. Nat Genet 38:688–693
36. Coutifaris C, Kao LC, Sehdev HM et al (1991) E-cadherin expression during the differentiation of human trophoblasts. Development 113:767–777
37. Dessimoz J, Bonnard C, Huelsken J, Grapin-Botton A (2005) Pancreas-specific deletion of beta-catenin reveals Wnt-dependent and Wnt-independent functions during development. Curr Biol 15:1677–1683
38. Rulifson IC, Karnik SK, Heiser PW et al (2007) Wnt signaling regulates pancreatic beta cell proliferation. Proc Natl Acad Sci USA 104:6247–6252
39. Murtaugh LC, Law AC, Dor Y, Melton DA (2005) Beta-catenin is essential for pancreatic acinar but not islet development. Development 132:4663–4674
40. Chen H, Gu X, Liu Y et al (2011) PDGF signalling controls age-dependent proliferation in pancreatic beta-cells. Nature 478:349–355
41. Eberhard D, Kragl M, Lammert E (2010) 'Giving and taking': endothelial and beta-cells in the islets of Langerhans. Trends Endocrinol Metab 21:457–463
42. Head WS, Orseth ML, Nunemaker CS, Satin LS, Piston DW, Benninger RK (2012) Connexin-36 gap junctions regulate in vivo first- and second-phase insulin secretion dynamics and glucose tolerance in the conscious mouse. Diabetes 61:1700–1707
43. Konstantinova I, Nikolova G, Ohara-Imaizumi M et al (2007) EphA-Ephrin-A-mediated beta cell communication regulates insulin secretion from pancreatic islets. Cell 129:359–370
44. Parnaud G, Gonelle-Gispert C, Morel P et al (2011) Cadherin engagement protects human beta-cells from apoptosis. Endocrinology 152:4601–4609
45. Concannon P, Erlich HA, Julier C et al (2005) Type 1 diabetes: evidence for susceptibility loci from four genome-wide linkage scans in 1,435 multiplex families. Diabetes 54:2995–3001